JOURNAL OF INVERTEBRATE PATHOLOGY 63, 43–55 (1994)

Dimensions, Density, and Settling Velocity of Entomophthoralean Conidia: Implications for Aerial Dissemination of Spores

A. J. SAWYER,* M. H. GRIGGS,† AND R. WAYNE‡

*Plant Protection Research Unit, USDA–ARS, Tower Road, Ithaca, New York 14853; †Department of Entomology, Cornell University, Ithaca, New York 14853; and ‡Section of Plant Biology, Cornell University, Ithaca, New York 14853

Received December 9, 1992; accepted May 3, 1993

The epizootic behavior of entomopathogens is determined, in part, by their capacity for spatial spread in a host population. Among the entomophthoralean fungi, this may be accomplished through various mechanisms, including passive aerial dissemination of conidia. In this study we measured the size, shape, density, and settling velocity in still air of conidia of three species of entomophthoralean fungi: *Zoophthora radicans, Conidiobolus obscurus,* and *Conidiobolus thromboides.* In addition, the aerodynamic behavior of *Z. radicans* conidia was observed. Size and shape, measured by light microscopy, were consistent with previously reported values. Conidial densities (1.10 g cm^{-3} for *Z. radicans* and 1.06 g cm^{-3} for *Conidiobolus* spp.) were determined from the refractive index of spores measured by interference microscopy; these are the first reports in the literature of the density of entomophthoralean conidia. Settling velocity was measured by allowing fungal cultures to sporulate into a glass chamber, while falling conidia were observed by video microscopy. Images of falling spores were analyzed by a computerized motion analysis system, and settling velocities were determined. The system was calibrated by measuring the settling velocity of polystyrene microspheres of sizes similar to those of the spores and comparing observed velocities to those predicted by Stokes' Law. These are the first reports of settling velocity for entomophthoralean conidia. The nearly spherical spores of *C. thromboides* fell at velocities expected from Stokes' Law (median, 1.4 cm sec^{-1}), while the spherical, but larger, spores of *C. obscurus* fell more slowly than expected (median, 4.6 cm sec^{-1}), for reasons that are unclear. Conidia of *Z. radicans* fell at a velocity equal to that of spheres of the same volume and density (median, 0.4 cm sec^{-1}), with little or no correction needed for their ellipsoidal shape. The settling velocity of ellipsoidal particles depends on their orientation. The falling orientation and aerodynamic behavior of conidia of *Z. radicans* were observed by high-resolution video microscopy; the spores consistently fell in a stable orientation with their major axis vertical. Our measurements of conidial size, shape, density, and settling velocity in still air provide information needed for models of particulate transport, which can be used to predict spore dispersal under field conditions involving wind and turbulence above and within plant canopies. © 1994 Academic Press, Inc.

KEY WORDS: **Zygomycetes: Entomophthorales; *Zoophthora radicans; Conidiobolus thromboides; Conidiobolus obscurus;* fungal pathogen; conidium; spore; dispersal.**

INTRODUCTION

Biological Background

Dispersal plays a central role in the ecology and epizootiology of insect pathogens (Tanada, 1963; Glare and Milner, 1991). As it does for other organisms, dispersal allows pathogens to utilize spatially discontinuous or ephemeral resources, colonize vacant habitats, and participate in genetic mixing. Dispersal is also an essential component of disease transmission, enabling pathogens to bridge the space separating them from prospective hosts. The behavior of epizootics is determined, in large part, by the capacity of pathogens for spatial spread. The importance of pathogen dispersal to epidemiology has been studied extensively by plant pathologists (Meredith, 1973; Zadoks and Schein, 1979; Leonard and Fry, 1986; Jeger, 1989). Yet, with few exceptions (Entwhistle *et al.,* 1983; Onstad and Maddox, 1989; Dwyer, 1992), the subject has remained a neglected aspect of insect pathology (Carruthers and Soper, 1987).

Entomophthoralean fungi are dispersed by several mechanisms (MacLeod, 1963; Ingold, 1971). Conidia are forcibly discharged from host cadavers, which, by itself, results in displacement of only a centimeter or so. Should these primary conidia fail to contact a suitable host, they may produce and discharge secondary conidia or, in some species, form stalked, adhesive capilliconidia that may be picked up by a passing host. Movement of infected hosts results in greater displacement. Infection by some fungi causes insect hosts to climb to elevated positions on plants and become attached, aiding aerial dissemination of conidia. Dis-

0022-2011/94 $5.00

eased insects usually move about for some time before death, carrying the pathogen with them—in a few cases even dispensing conidia as they go. Rain splashes and water flow on plant surfaces may disperse conidia and resting spores.

Due to the recognized importance of aerial dissemination in the epidemiology of phytopathogenic fungi, a number of studies have been made of the release, dispersal, and deposition of spores of rusts, mildews, and other fungal pathogens of plants (Aylor, 1978; Berger and Luke, 1979; Fitt *et al.*, 1987; McCartney and Bainbridge, 1987; Aylor and Ferrandino, 1989; McCartney, 1991). Aerial dispersal of *Lycopodium* spores, pollen, spray droplets, smoke, and dust has also been studied experimentally and in theoretical treatments and models (Green and Lane, 1964; Chamberlain and Chadwick, 1972; Aylor, 1975; Parkin and Merritt, 1988; Okubo and Levin, 1989). There have been no studies of the aerial dynamics of entomopathogenic fungi, although the incidence of entomophthoralean conidia in the air has been reported (Wilding, 1970).

The purpose of the present study was to obtain physical measurements basic to the understanding of aerial dispersal by certain entomophthoralean conidia. We measured the size, shape, density, and settling velocity in still air of primary conidia of *Zoophthora radicans*, *Conidiobolus obscurus*, and *Conidiobolus thromboides*. In addition, the aerodynamic behavior of *Z. radicans* conidia settling in still air was observed. *Z. radicans* is a candidate biological control agent for leafhoppers and the subject of ongoing research in our laboratory. *C. obscurus* and *C. thromboides* were added to the study for comparative purposes, possessing conidia which differ in size and shape from those of *Z. radicans*. The information obtained in this study can be used in existing models of particulate transport to predict spore dispersal under field conditions involving wind and turbulence above and within plant canopies (Legg and Powell, 1979; McCartney and Fitt, 1985; DiGiovanni *et al.*, 1989; Aylor, 1990; de Jong *et al.*, 1991). Ultimately, this will improve our understanding of the spatial dynamics of fungal epizootics in insect populations and aid in devising strategies for deploying fungal pathogens as microbial control agents of insect pests.

Physical Theory

The focus of this paper is on aerial dissemination of primary conidia. Although forcible discharge can disperse conidia a short distance, its main function may be to get spores out of the boundary layer of still air surrounding the cadaver and plant surface and into a moving air stream (Gregory, 1945). Once airborne, conidia settle by gravitation but may also be carried horizontally and vertically by wind. Ultimately they become deposited on surfaces by sedimentation and impaction (Chamberlain, 1967; Gregory and Monteith, 1967). Many factors influence the movement of conidia through air. A major consideration is their small size: particles with diameters <100 μm, including most fungal spores, undergo the "creeping motion" of low Reynolds number fluid dynamics (Vogel, 1981). Although air does not seem to be a viscous medium in our everyday experience, to a spore it is very much so. The Reynolds number (R_e) of a fluid system is a dimensionless parameter representing the ratio of inertial to viscous forces, and thus provides a qualitative indication of the nature of an object's motion through the fluid:

$$R_e = \frac{LV\rho_f}{\mu}, \tag{1}$$

where L (in cm) is the length of the object in the direction of motion, V is its velocity (in cm sec^{-1}) ρ_f is the density of the fluid (in g cm^{-3}), and μ is the dynamic viscosity of the fluid (in g cm^{-1} sec^{-1}). For air at 20°C, $\rho_f = 1.2 \times 10^{-3}$ g cm^{-3} and $\mu = 1.8 \times 10^{-4}$ g cm^{-1} sec^{-1}. In still air at 20°C, a 15-μm-diameter smooth sphere with a density of 1 g cm^{-3} falls at a terminal velocity of 0.68 cm sec^{-1}. R_e in this example is 0.007, placing this motion well within the realm of fluid dynamics dominated by viscous forces.

For $R_e < 1.0$, Stokes' Law gives the drag, F_d (in dynes), on a spherical particle of radius r (in cm) as

$$F_d = 6\pi r\mu V. \tag{2}$$

A falling spherical particle accelerates until the increasing drag equals the force of gravity ($mg = \frac{4}{3}\pi r^3(\rho_p - \rho_f)g$), after which the particle falls at terminal, or Stokes' velocity, V_s. Setting $F_d = mg$ and solving for V_s we obtain:

$$V_S = \frac{2}{9} r^2 g \left(\frac{\rho_p - \rho_f}{\mu}\right), \tag{3}$$

where g (= 981 cm s^{-2}) is the acceleration due to gravity and ρ_p is the density of the particle (in g cm^{-3}). The ratio of the terminal velocity to the acceleration due to gravity is called the relaxation time, τ (in sec):

$$\tau = \frac{2}{9} r^2 \left(\frac{\rho_p - \rho_f}{\mu}\right). \tag{4}$$

The relaxation time characterizes how quickly viscous forces act to slow a particle ejected forcefully into still air. A particle projected with horizontal velocity V_0 travels a distance S (in cm)

$$S = \tau V_0, \tag{5}$$

called the stopping distance, before its horizontal motion is stopped by the drag of the air (Davies, 1966b). For example, a 15-μm spherical spore discharged with an initial velocity of 15 m sec^{-1} would travel only 1 cm before coming to a stop and falling vertically at terminal velocity; this would happen within a few milliseconds.

A number of other factors affect the rate at which a spore settles in still air. The viscosity of air varies slightly over the range of temperatures of interest in aerobiology (1.7×10^{-4} g cm^{-1} sec^{-1} at 0°C to 1.9×10^{-4} g cm^{-1} sec^{-1} at 40°C) (Weast, 1983, p. F-43). The density of air varies with temperature and moisture content, but while this influences R_e (Eq. 1), it does not affect the drag on a particle moving through air within the Stokes' realm (Eq. 2). Small particles may be subject to forces other than gravity and viscous drag. Most small particles, including spores, carry a net electrical charge; this may influence their deposition on surfaces, but is likely to be important only over distances of a few millimeters (Gregory, 1945). Small particles move along temperature gradients (thermophoresis) and diffusion gradients (diffusiophoresis) and may move toward or away from a light source (photophoresis). These small forces are unlikely to be important in spore dispersal under natural conditions, but may complicate laboratory studies (Gregory, 1945; Davies, 1966a; Webster *et al.*, 1988). Boundary layers—zones around objects in which fluid motion is significantly impeded by viscous drag—may slow a particle falling near a wall or other surface; at low R_e this effect may extend to hundreds or thousands of times a particle's diameter (White, 1946; Vogel, 1981).

Properties of the spore itself greatly affect its aerodynamic behavior. As Eq. 3 indicates, settling velocity increases with the square of a particle's radius and in proportion to the difference between its density and that of air. Equation 2, giving the drag on a particle at low R_e, applies only to smooth spheres. Many fungal spores, while not spheres, are approximately ellipsoids, the one other shape for which drag coefficients have been determined theoretically (Fuchs, 1964). The orientation of elongate particles during settling greatly affects the drag they experience. A prolate ellipsoid with a 3:1 ratio of length to width, falling with its major axis parallel to the direction of motion, has a terminal velocity 3% greater than that of a sphere of the same volume and density. This same ellipsoid, falling with its long axis horizontal, would have a velocity only 83% of that of a sphere of the same volume. The settling orientation of an elongate, symmetrical particle of uniform density depends on the R_e describing that particle's motion. At low R_e (<0.05–0.1), any initial orientation is stable, whereas at higher R_e, symmetrical, homogeneous particles begin to orient so that drag is maximized; i.e., an elongate particle falls with its long axis horizontal. However, asymmetry or a nonhomogeneous distribution of mass may cause an elongate particle to fall with a vertical orientation, reducing drag and increasing its velocity (Fuchs, 1964). The irregular surfaces of many pollen grains and fungal spores may also increase the drag they experience (Gregory, 1945, 1973; Burrows, 1986; Latgé *et al.*, 1989).

The shapes and sizes of entomophthoralean conidia vary considerably, from the small campanulate spores of *Entomophthora culicis* (11 × 13 μm), to the large, nearly spherical conidia of *Batkoa major* (47 × 50 μm) and the elongate, fusiform spores of *Erynia gracilis* (8 × 40 μm). Of those species used in the present study, primary conidia are ellipsoidal (*Zoophthora radicans*, 7.6 × 19.5 μm) or nearly spherical (*C. thromboides*, 23 × 27 μm; *C. obscurus*, 32 × 39 μm) (Waterhouse and Brady, 1982). Measured dimensions may depend on preparation techniques (Beckett *et al.*, 1984). Densities of entomophthoralean conidia have not been reported, but the spores of other species of fungi range in density from 0.56 to 1.36 g cm^{-3}, commonly 1.1 to 1.2 g cm^{-3} (Gregory, 1973).

MATERIALS AND METHODS

Sources and Culture of Fungi

Cultures of *Z. radicans* (ARSEF 2282 and 2283), *C. obscurus* (ARSEF 74), and *C. thromboides* (ARSEF 40) were obtained from the USDA–ARS Collection of Entomopathogenic Fungal Cultures in Ithaca, New York (Humber, 1992). Fungi were grown on Sabouraud dextrose agar with yeast (SDAY = 40 g dextrose, 10 g peptone, 10 g yeast extract, 15 g agar in 1 liter of water) at room temperature. Sections of actively growing fungus from *Z. radicans* cultures provided inoculum for producing large quantities of dried mycelium by the method of McCabe and Soper (1985). As needed, small fragments of dry mycelium were rehydrated on water agar at 10°C for 16 hr, bringing the fungus to the point of conidial sporulation. Cultures of *Conidiobolus* spp. were scraped from SDAY and also placed on water agar at 10°C for 16 hr to induce conidiogenesis. A few hours before spores were needed, cultures on water agar were brought to room temperature and inverted over water-saturated filter paper to encourage sporulation.

Size, Shape, and Density of Conidia

Conidia are highly responsive to changes in water potential, swelling rapidly in distilled water and shriveling on dry glass. Because settling velocity depends on spore size, shape, and density, these properties must be measured under conditions duplicating as nearly as possible the water potential of the humid aerial environment in which conidia are normally produced and discharged. Conidia showered into lactophenol (20 g phenol, 17.5 ml lactic acid, 35.4 ml glycerol, 20 ml

distilled water) showed no evidence of swelling or shrinking compared to fresh spores showered from cultures growing on water agar onto glass in a small closed dish having a saturated atmosphere. Therefore, we measured the dimensions (length and width) of conidia in lactophenol, using a compound microscope (500×) equipped with a calibrated ocular micrometer and bright-field optics. Approximately 100 conidia of each fungal isolate were measured (59 for *Z. radicans* isolate 2282).

Conidial densities were determined by interference microscopy (Barer and Joseph, 1958; Wayne and Staves, 1991). The method is based on the fact that the refractive index of a cell depends on the concentration of dissolved solids (e.g., proteins) that it contains. The method is rapid and accurate and has the advantage of providing estimates of density for individual spores. Spores were immersed in 25% glycerol (refractive index, 1.3637), an isotonic medium in which they retained their natural shapes, and were observed at a wavelength of 550 nm using a Zeiss Jamin–Lebedeff interference microscope with a 40× objective lens (NA = 0.65). The phase was adjusted to give maximum contrast between the conidium, taken as a whole, and the immersion medium. The observed phase difference and the optical path length (width of the spore at its center) were used to calculate the spore's solid concentration, C (in g cm^{-3}). Assuming that the organic dry matter is mostly protein, we then calculated the spore's density (in g cm^{-3}) as $\rho = C + (1 - vC)$, where v is the specific volume of protein, 0.75, and $(1 - vC)$ is the spore's water concentration (in g cm^{-3}). Densities were determined for approximately 20 conidia of each fungal isolate.

Settling Velocity

Experimental approach and apparatus. Settling velocities of conidia in still air were measured directly by observing spores falling in a glass chamber by video camera and analyzing images with a computerized motion analysis system. The size of the chamber, 15.0 × 2.3 × 2.5 cm ($H \times W \times D$), was a compromise between the need to eliminate convection currents, which could not be controlled in larger chambers, and an effort to minimize wall effects, which may slow the settling of particles by viscous drag (see below). Cultures of fungus sporulating on water agar were inverted over the chamber; discharged conidia fell through a hole cut in the lid of a petri dish glued to the top. Distilled water in the bottom of the chamber maintained relative humidity >85% at room temperature, as shown in tests with an RH sensor (Model PCRC-11, PhysChem, Inc.) placed in the chamber. The chamber was allowed to equilibrate for several hours before beginning observations. To provide thermal stability and darken the photographic arena, the glass chamber was enclosed in a styrofoam box, 30 × 11.5 × 15 cm ($H \times W \times D$), lined with black paper. An aperture at the front admitted the photographic lens, and holes were provided at the back for two light sources. A thermistor probe was inserted into the enclosure to record temperature during observations.

Two light beams (2 cm diameter) crossing at an angle of ca. 60° in the center of the chamber created a dark-field effect, in which illuminated spores appeared brightly lit against a dark background. A fiber optic light source was used to reduce heating; a series of glass lenses focused the beams and filtered out IR radiation; red filters further limited the light to wavelengths near the peak sensitivity of the video camera (700 nm). Light intensity was set to the lowest level that would permit imaging.

A CCD video camera (Model 6410, Cohu, Inc., San Diego, CA) equipped with a 2× macrofocusing teleconverter, a 52-mm, f4.5 macrozoom lens (70–210 mm), and three close-up attachment lens (1×, 2×, and 3× diopters) (Vivitar, Inc.), provided a high-resolution, light-sensitive imaging system (total magnification, 46×). The camera was leveled with a spirit level and oriented to provide the greatest resolution (774 pixels) in the vertical direction. The image was then digitized with a Motion Analysis VP110 video processor (Motion Analysis Corp., Santa Rosa, CA) and analyzed by an Amdek System 386 microcomputer (Amdek, San Jose, CA) using customized computer programs (available upon request). Video fields were collected every 1/60 sec. The field of view was typically 0.55 cm in the vertical direction. The usable depth of field was estimated to be ca. 0.55 cm as well, with nearer or farther objects becoming increasingly out of focus outside of this range. The camera was focused on the center of the chamber, equidistant from the four walls.

Measurement of settling velocity. Falling spores were observed for intervals of 5 to 60 sec, depending on sporulation rates, to collect a number of images that could be handled efficiently by the video processor. In each video field, the processor identified objects of interest and generated points on the computer screen representing their centroids. Centroids in successive fields were associated with each other by the processor and interpreted as moving objects, for which velocity was calculated automatically based on a measured scaling factor, typically 21.5 μm/pixel, and the scanning speed of 60 fields sec^{-1}. Program parameters were adjusted to exclude out-of-focus objects and objects apparently moving too slowly to be spores (dust, droplets of fluid ejected from rupturing conidiophores, or debris adhering to the walls of the chamber), too rapidly (presumably clusters of two or more conidia), or at an angle that departed >5° from the vertical (generally due to the processor joining unrelated centroids). Preliminary measurements made at distances of 3, 5, 7, and 9 cm from the top of the chamber showed that falling spores had already reached terminal velocity within 3 cm of

the point of discharge. Subsequently, all observations were made at 5 cm. Velocities calculated by the motion analysis system for individual segments of trajectories also showed no evidence of acceleration.

Estimation of wall effects. As noted, a small chamber was used to eliminate convection currents which would interfere with measurements of settling velocity. However, at low R_e, the viscous drag associated with boundary layers can slow objects moving near walls or other objects (White, 1946; Vogel, 1981, p. 249). To evaluate the influence of the chamber walls on the motion of falling particles in our apparatus, we compared the observed terminal velocities of smooth spherical particles to those predicted by Stokes' Law (Eq. 3). We obtained dry polystyrene microspheres (ρ = 1.05 g cm^{-3}) in nominal sizes of 13, 15, 20, 26, and 49 μm (mean diameter weighted by volume) (Bangs Laboratories, Inc., Carmel, IN). Particles were dispensed at the top of the observation chamber from a small container attached to an electronic "shaker," constructed from a small speaker and oscillator circuit. Settling velocities were determined as they were for conidia; the only differences in procedure were that microspheres were collected at the bottom of the chamber for measurement of sizes actually dispensed, and no water was placed in the bottom of the chamber.

Analysis of settling velocities. Observed settling velocities of conidia and polystyrene microspheres were compared to those predicted by Stokes' Law for spheres of the same volume and density. This required paired measurements of particle size and velocity. The small size of images analyzed by the video system did not permit direct measurements of the particles as they were observed in the settling chamber. Rather, a statistical approach was taken to associating particle sizes and velocity measurements. For microspheres, 100 particles of each nominal size were randomly selected from those collected in the bottom of the settling chamber and were measured at 500× under a light microscope. Conidial sizes were measured separately, as described above, rather than by collecting spores at the bottom of the chamber. However, these separate spores were from the same cultures used to study settling velocity and were measured at the same time. Deciles were then computed from the distributions of sizes and velocities, and corresponding deciles (10th percentile . . . 90th percentile) were matched. Assumptions underlying this procedure were that velocity and size measurements were taken without bias from the same populations, and that sample sizes were large enough to provide good representations of both size and velocity.

Calculations of expected velocity used values for the viscosity and density of air adjusted for temperature, as measured in the settling chamber at the time of observation. The mean observed density of conidia for each fungal isolate and the density reported by the manufacturer of the polystyrene microspheres were used in the calculations. Expected velocities were based on the assumption that polystyrene microspheres and conidia of *Conidiobolus* spp. were spheres, for which Stokes' Law applies directly. For conidia of *Conidiobolus* spp., diameter was estimated as $(L + W)/2$, where L, length and W, width. Conidia of *Z. radicans* were assumed to be prolate ellipsoids, for which the diameter of a sphere of equal volume is given by $d = \sqrt[3]{LW^2}$.

When comparing observed and expected velocities, a number of complications arose. First, some observed velocities were greater than would be expected, by Stokes' Law, for a sphere of the same volume as the largest measured particle or spore. We assumed that these represented aggregates of two or more microspheres or conidia and discarded them before computing deciles for velocity. This eliminated 4.7% of the observations of microsphere velocity and 1.6% of the observations of conidial velocity. (For conidia of *Z. radicans,* allowance was made for the fact that a short ellipsoid oriented vertically may fall as much as 5% faster than a sphere of the same volume (Fuchs, 1964); therefore, for these conidia, only those observations exceeding 105% of the velocity expected for a sphere of the same volume as the largest measured spore were discarded.)

Second, the largest microspheres and conidia of *C. obscurus* fell fast enough to require the application of Oseen's correction to Stokes' Law when computing expected velocities. Oseen's correction, an empirical relationship, reduces the expected velocity to approximately $V_s/(1 + \frac{3}{16}R_e)$ to account for increased drag due to turbulence at larger R_e (Chatigny *et al.,* 1979). Oseen's correction $(1 + \frac{3}{16}R_e)$ for the largest microsphere was 1.21, and for the largest conidium of *C. obscurus* it was 1.06.

Finally, 3% of the large particles (nominally 49 μm) and 2% of *C. obscurus* spores were large enough to fall too fast for the video processor to capture, with the parameter values used in those runs. In these cases, before computing deciles for size, the lists of measured sizes were truncated at diameters corresponding to the largest observed velocities, based on Stokes' Law with Oseen's correction.

Settling Orientation and Aerodynamic Behavior of Z. radicans *Conidia*

Theoretical calculations indicate that prolate ellipsoids fall with a velocity that differs from that of a sphere of equal volume, depending on the ratio of length to width and on settling orientation (Fuchs, 1964, p. 40; Vogel, 1981, p. 248). Moreover, motions such as rotation and autogyration can slow the descent of seeds and other falling objects, as the available energy is partitioned into rotational as well as transla-

tional motion (Vogel, 1981; Burrows, 1986; Niklas, 1992). Therefore, the orientation and aerodynamic behavior of conidia of *Z. radicans* during settling were of interest. Conidia of *Z. radicans* (ARSEF 2283) were observed as they fell in still air in the same chamber used to measure settling velocity. In this case, however, the video camera was attached to a horizontally mounted Olympus BH-2 compound microscope, with 4× objective, 15× wide-angle photo eyepiece and 5.8× camera adapter (total magnification, 350×). Images were recorded on broadcast-quality videotape with a time lapse recorder (Model AG-6720A, Panasonic, Inc.) at a rate of 60 fields sec^{-1}. Recorded trajectories were examined frame by frame, and images of individual conidia were analyzed for angle of trajectory (with respect to vertical), and angle of the spore's major axis (with respect to the line of trajectory). A protractor was used to measure angles on the screen, with the help of horizontal and vertical guidelines generated by an attached video analyzer. The trajectories of 49 conidia were analyzed, with 3–18 images per trajectory.

RESULTS

Size, Shape, and Density of Conidia

Conidia of *Z. radicans* were approximately ellipsoidal (Fig. 1A), with a ratio of length to width ranging from 1.9 to 3.7, averaging 2.6–2.8 (Table 1). Spores of isolate 2282 were slightly smaller than those of isolate 2283 (*t* test on estimated diameters of spheres of same volume, $P < 0.05$). Conidia of *Conidiobolus* spp. were spherical, with a basal papilla (Figs. 1B and 1C). For all isolates, sizes varied moderately, with coefficients of variation (CV = SD/mean) of 7–13%. The observed shapes and size ranges of conidia were similar to those reported in the literature (Thaxter, 1888; Waterhouse and Brady, 1982).

The density of conidia of *Z. radicans* averaged 1.10 g cm^{-3}, while the density of spores of *Conidiobolus* spp. averaged slightly less, 1.06 g cm^{-3} (Table 2). Densities were quite uniform within each isolate (CV < 1%).

Settling Velocity

The actual sizes of polystyrene microspheres collected in the bottom of the settling chamber are reported in Table 3. The observed mean sizes differed from those given by the manufacturer, which were calculated in a different way. Through its mechanical action, our dispensing device may also have selected a different distribution of particle sizes than that of the bulk sample supplied by the manufacturer.

Observed velocities of microspheres and conidia are summarized in Table 4. The smaller polystyrene mi-

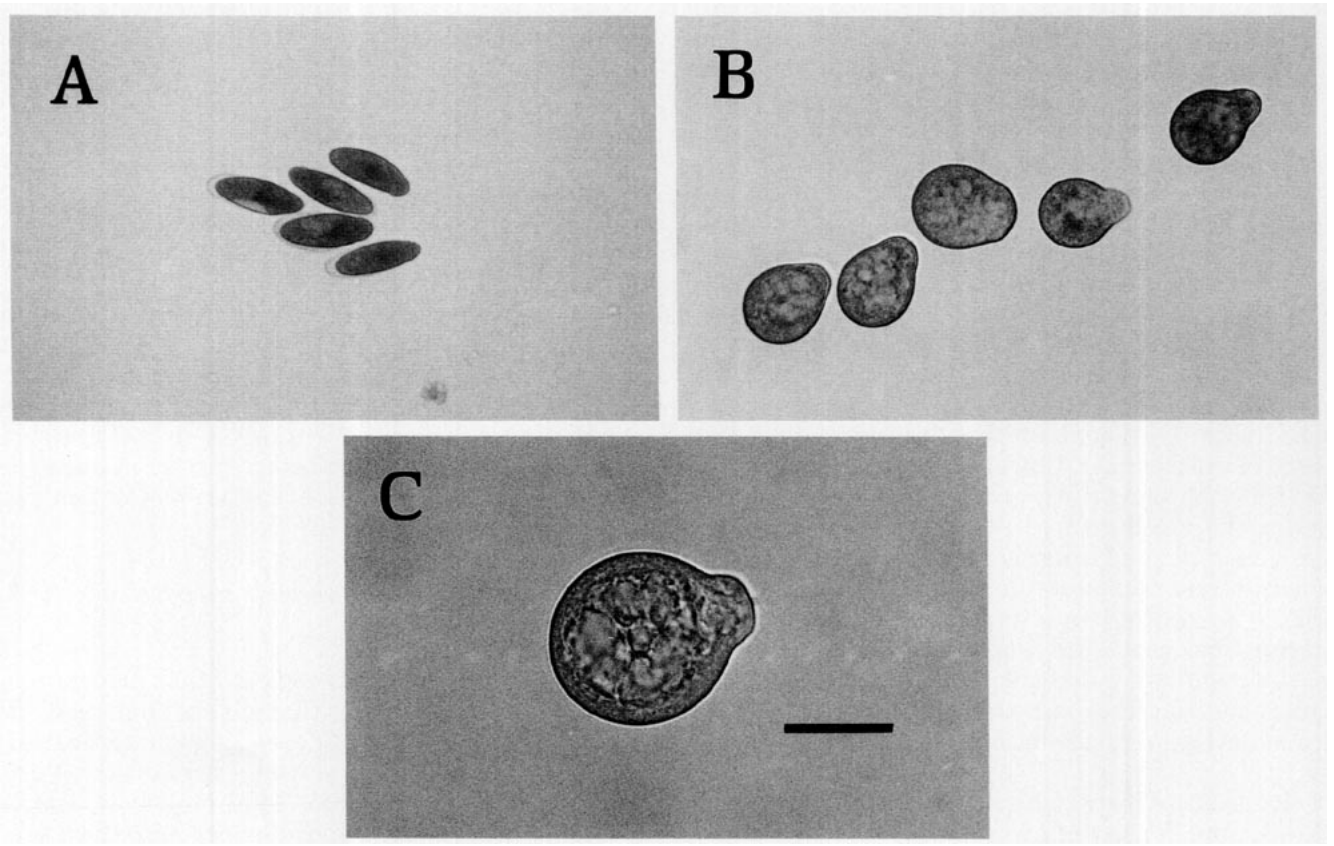

FIG. 1. Photomicrographs of conidia of *Z. radicans* (A), *C. thromboides* (B), and *C. obscurus* (C) in lactophenol (scale bar, 25 μm).

TABLE 1
Dimensions of Conidia

Species: Isolate[a]:	*Z. radicans* 2282	*Z. radicans* 2283	*C. thromboides* 40	*C. obscurus* 74
Length (L), μm				
Mean	19.7	21.4	23.0	47.8
SD	1.38	1.39	1.95	6.23
Range	17.1–22.9	17.6–27.3	19.4–29.7	34.3–60.0
Width (W), μm				
Mean	7.5	7.6	18.4	40.4
SD	0.77	0.72	1.68	5.80
Range	6.3–9.1	6.8–9.7	15.4–23.4	26.3–58.3
L/W				
Mean	2.6	2.8	1.3	1.2
SD	0.29	0.29	0.08	0.08
Range	1.9–3.3	2.3–3.7	1.0–1.5	0.8–1.4
Equivalent diameter, μm[b]				
Mean	10.4	10.7	20.7	44.1
SD	0.79	0.77	1.70	5.77
Range	9.3–12.2	9.3–13.7	17.4–26.3	31.4–57.2
No. measured	59	100	96	100

[a] ARSEF accession No.
[b] Diameter of sphere of same volume: for *Z. radicans*, $\sqrt[3]{LW^2}$; for *Conidiobolus* spp., $(L + W)/2$ (see text).

crospheres (13, 15, 20, 26 μm) all fell at terminal velocities predicted very well by Stokes' Law (Fig. 2A). However, the largest microspheres (49 μm) fell more slowly than expected, even with Oseen's correction for turbulent drag taken into consideration (Fig. 2B).

Conidia of *C. thromboides* fell at a terminal velocity perfectly predicted by Stokes' Law (Fig. 3A), with a median rate of 1.4 cm sec^{-1}. However, the larger conidia of *C. obscurus* fell more slowly than expected, even with Oseen's correction taken into account (median velocity, 4.6 cm sec^{-1}) (Fig. 3B, closed circles). If width alone, rather than $(L + W)/2$, was used as a measure of spore size for *C. obscurus*, then observed settling velocities were close to those expected for spheres of the same volume; indeed, the median observed velocity was nearly equal to the predicted value (Fig. 3B, open circles). For *Z. radicans*, median observed settling velocities for both isolates (0.34 cm sec^{-1}) were as predicted by Stokes' Law for spheres of the same volume. However, velocities increased with size more rapidly than expected (Fig. 3C). Because the L/W ratio of ellipsoids is known to affect drag (Fuchs, 1964), we examined the relationship between conidial size and shape. Combining measurements on both isolates of *Z. radicans*, we found a significant negative correlation ($r = -0.44$, $P < 0.01$, $df = 157$) between L/W and $d = \sqrt[3]{LW^2}$, the diameter of a sphere of the same volume as the ellipsoid representing the spore; i.e., smaller spores were more elongate. Based on the regression $L/W = 4.56 - 0.17d$, a dynamic shape factor (DSF) was calculated for prolate ellipsoids falling with a vertical orientation (see next section) (Fuchs, 1964). The dotted line in Fig. 3C is V_s/DSF. For $d = 9$ μm, $L/W = 3.0$ and DSF = 0.97. For $d = 12$ μm, $L/W = 2.5$ and DSF = 0.96. The small difference in shape of conidia was insufficient to account for the apparent increase in velocity with size.

TABLE 2
Density of Conidia

Species: Isolate[a]:	*Z. radicans* 2282	*Z. radicans* 2283	*C. thromboides* 40	*C. obscurus* 74
Density, g cm^{-3}				
Mean	1.098	1.098	1.061	1.055
SD	0.0059	0.0100	0.0014	0.0017
Range	1.088–1.112	1.087–1.129	1.059–1.063	1.051–1.057
No. measured	20	21	20	17

[a] ARSEF accession No.

TABLE 3
Diameter of Polystyrene Microspheres Dispensed into the Settling Chamber

	Nominal size (μm)				
	13	15	20	26	49
Mean, μm	13.0	19.7	20.4	24.9	62.1
SD	1.92	2.56	2.93	3.50	6.23
Range	9.1–18.2	15.0–26.7	11.1–26.7	15.3–33.5	49.0–82.4[a]
No. measured	100	100	100	100	97

[a] Maximum size corresponds to the largest particle whose velocity could be measured by the motion analysis system.

Settling Orientation and Aerodynamic Behavior of Z. radicans *Conidia*

In observations made by high-resolution video microscopy, conidia of *Z. radicans* were always seen to fall in a vertical orientation (Fig. 4 shows typical flight behavior). Of 49 conidia observed, 21 fell with no measurable departure of the spore's longitudinal axis from the downward path of its trajectory (Fig. 5). Others fell with the axis at a slight, sometimes varying, angle from the line of flight. Overall, the mean absolute

TABLE 4
Velocity of Polystyrene Microspheres and Fungal Conidia

Subject	Velocity, cm sec^{-1} Mean	SD	Range	No.
Microspheres[a]				
13 μm	0.52	0.163	0.20–0.97[c]	406
15 μm	1.24	0.388	0.36–2.20[c]	402
20 μm	1.17	0.437	0.35–2.20[c]	337
26 μm	2.00	0.562	0.65–3.47[c]	300
49 μm	8.88	2.406	2.99–17.5	230
Conidia[b]				
Z. radicans, 2282	0.36	0.096	0.10–0.63[c]	129
Z. radicans, 2283	0.37	0.119	0.11–0.64[c]	128
C. thromboides, 40	1.39	0.207	0.99–2.07[c]	245
C. obscurus, 74	4.49	1.230	1.05–8.84	275

[a] Nominal size.
[b] Species, ARSEF accession No.
[c] Velocities truncated at maximum expected for largest measured particle or spore.

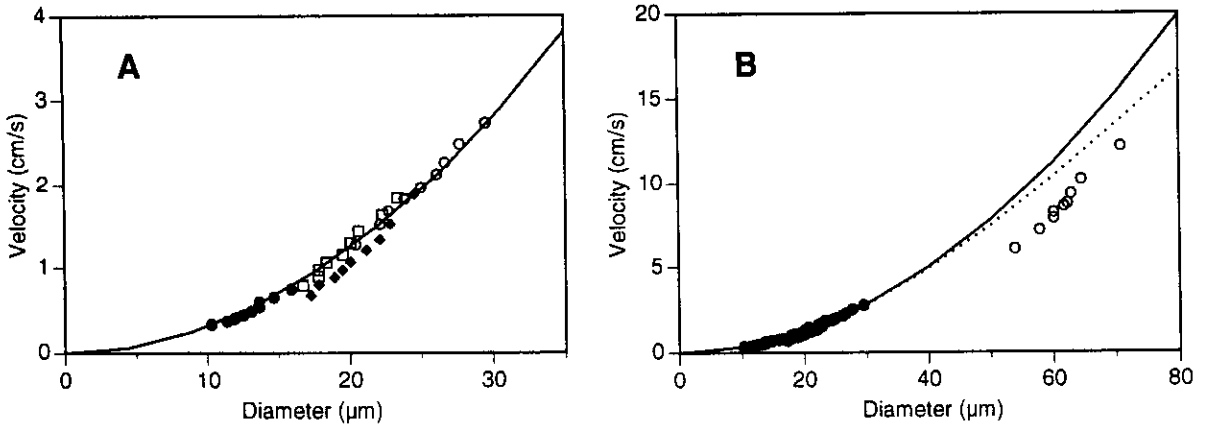

FIG. 2. Settling velocity of polystyrene microspheres vs particle diameter. Symbols: measured sizes and observed velocities paired at equal deciles (10th percentile–90th percentile). Solid lines, expected velocity according to Stokes' Law. (A) Small microspheres (13, 15, 20, 26 μm). (B) All microspheres. Solid circles, small microspheres (13–26 μm); open circles, large microspheres (49 μm). Broken line, expected velocity with Oseen's correction for turbulent drag.

value of these departures was <1° (maximum, 9°). Occasionally there was evidence of regular oscillations in a spore's attitude, with a frequency of 15–30 cycles sec^{-1}. The trajectories themselves departed from the vertical by a mean absolute value of 2° (maximum, 11°); 49% fell within 1° of the vertical.

DISCUSSION

The size, shape, and density of particles greatly influence their aerodynamic behavior. Of these, size is most important in determining the rate at which a particle settles in still air. Among entomophthoralean conidia, ranging in mean diameter from 10 to 50 μm,

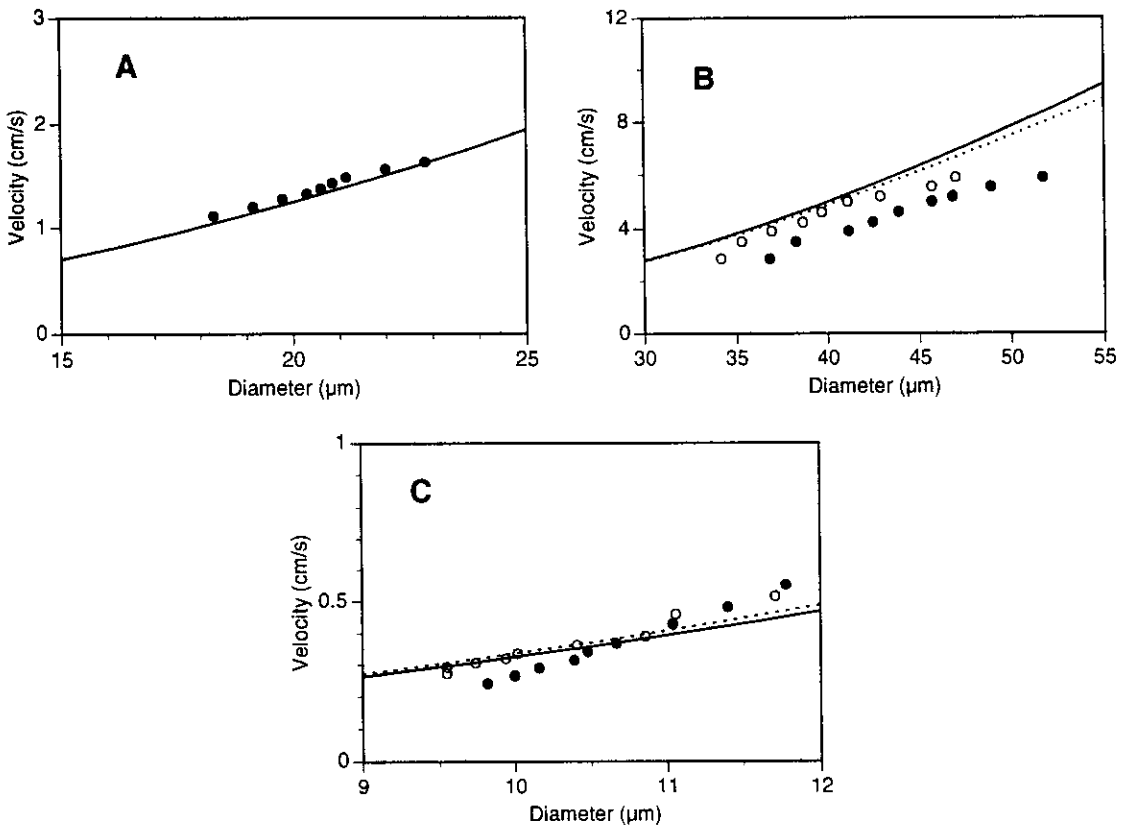

FIG. 3. Settling velocity of conidia vs diameter of sphere of same volume. Symbols, estimated sizes and observed velocities paired at equal deciles (10th percentile–90th percentile). Solid lines, expected velocity according to Stokes' Law. (A) *C. thromboides;* (B) *C. obscurus.* Solid circles, diameter estimated by $(L + W)/2$; open circles, diameter estimated by width alone. Broken line, expected velocity with Oseen's correction for turbulent drag. (C) *Z. radicans.* Solid circles, isolate 2283; open circles, isolate 2282. Broken line, expected velocity corrected for a size-dependent dynamic shape factor.

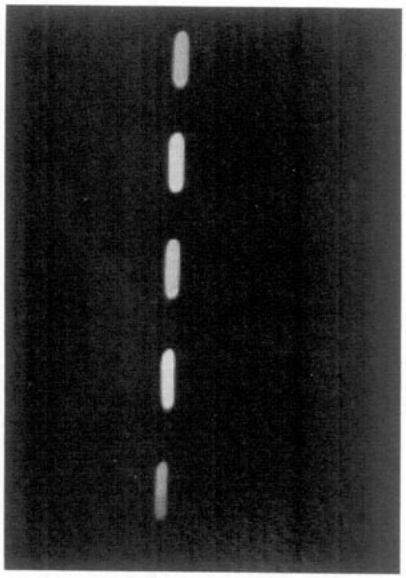

FIG. 4. Falling conidium of *Z. radicans*, showing typical downward trajectory and stable, vertical orientation of spore (multiple-exposure photograph of videotaped images, taken at intervals of 1/30 sec).

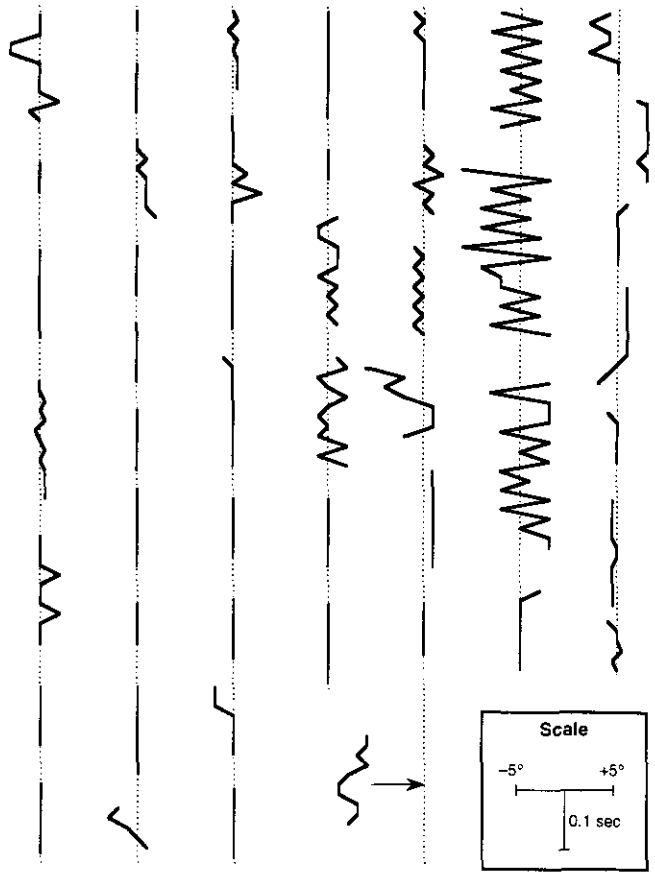

FIG. 5. Settling orientation and aerodynamic behavior of 49 conidia of *Z. radicans*. Dotted lines represent trajectories, solid lines indicate angles of departure of a spore's longitudinal axis from the trajectory as measured on videotaped images recorded at 60 frames sec^{-1}. Note the scale showing that variations in the attitude of falling conidia were generally <5°, indicating a stable, vertical orientation during settling.

size is clearly the most variable of the three factors. Due to the dependence of velocity on the square of particle radius (Eq. 3), median settling velocities can be expected to vary among species by a factor of 25×, from ca. 0.33 to 8.3 cm sec^{-1}. Even within a single isolate of one species, conidial size varies somewhat, as we found in the present study. It has been argued that the size, shape, and surface texture of fungal spores should be regarded as functional adaptations, modified by evolution to meet the requirements of liberation, dispersal, deposition, and survival (Ingold, 1971; Gregory, 1973). Uniformity of spore size within genera of airborne plant-pathogenic fungi has been noted and interpreted as an evolutionary compromise between a small size, favoring dispersal, and a large size, providing the nutrients needed for germination and haustorium formation (Matsumoto and Tajimi, 1985). Conidial size was at least as uniform within the isolates we examined as it was within the genera tabulated by Matsumoto and Tajimi (1985). The greater variation in sizes within the Entomophthorales as a whole may reflect constraints imposed by different life histories.

In contrast to size, the density of conidia was found to be remarkably uniform in the isolates we examined. This uniformity may reflect constraints on cellular content imposed by physiological requirements for spore survival or germination, rather than an optimal density for aerial dispersal. Some pollen grains and fungal spores that undergo long-distance aerial dispersal have buoyancy adaptations, such as air sacs and gas-filled vacuoles (Gregory, 1973), but these adaptations are apparently absent among the Entomophthorales. A possible source of error in our estimates of spore density was cellular heterogeneity, since conidia contain a nucleus, oil droplets, and other structures whose density differs from one another (Latgé *et al.*, 1989). To average out such differences, we reduced the spatial resolution of the interference microscope, and, in adjusting the phase, tried to maximize the contrast between the bulk of the spore and the surrounding medium. While there was an element of subjectivity involved in adjusting the phase, calculations show that a difference of ±5% in phase angle (approximately the bounds of uncertainty caused by observed variations in density within the spore) would lead to a difference of only ±0.25% in the estimate of density.

Conidial shape and surface texture enter into the equation as well: at the low R_e experienced by settling spores, departures from a spherical shape and smooth surface will generally increase drag and slow descent. However, the most extreme shape seen among entomophthoralean conidia (*E. gracilis*, 8 × 40 μm) is unlikely to reduce settling velocity by more than 30% from that of a sphere, even assuming that the spores

fall with a horizontal orientation (Fuchs, 1964). In our study, including a dynamic shape factor had a negligible influence on expected terminal velocities for the ellipsoidal conidia of *Z. radicans*. Surface texture (Latgé *et al.*, 1989) undoubtedly plays an even smaller role.

The dependency of a spore's dimensions on its state of hydration may have important implications, not only under experimental conditions, but in a natural setting as well. Pollen and fungal spores may begin to dehydrate immediately upon liberation, decreasing in density or size (Gregory, 1945, 1973). The result of dehydration would be a reduced settling velocity and increased likelihood of aerial dispersal. We have observed rapid and reversible changes in size and shape of *Z. radicans* conidia in response to changing water potential. Whether this effect might promote aerial dissemination by entomophthoralean conidia depends on how well these spores survive dehydration. In general, entomophthoralean conidia have been considered to be susceptible to desiccation (Carruthers and Soper, 1987; Glare and Milner, 1991). However, studies have shown that conidia can survive and remain infective for days or weeks at relative humidities of 40–50% (Brobyn *et al.*, 1987; Uziel and Kenneth, 1991).

The settling chamber used in our studies was small enough to eliminate convection currents and apparently large enough to avoid boundary layer effects that might have reduced the velocity of particles falling near walls. The smallest polystyrene microspheres (13, 15, 20, and 26 μm) all fell at terminal velocities predicted by Stokes' Law, showing that our apparatus and procedures were suitable for studying the aerodynamic behavior of conidia of similar size. However, the largest microspheres (49 μm) fell more slowly than expected. Based on empirical studies, the distance at which wall effects become negligible has been estimated to be 20 d/R_e, where d is the particle diameter (White, 1946; Vogel, 1981, p. 250). For the smallest microsphere we observed (d = 9 μm, V_s = 0.26 cm sec^{-1}, R_e = 0.002), this distance was 9.0 cm (10,000 diameters), while for the largest microsphere (d = 82 μm, V_s = 21.4 cm sec^{-1}, R_e = 1.17), it was only 0.14 cm (17 diameters). Thus, wall effects would not appear to account for the failure of the largest particles to obey Stokes' Law in our settling chamber, where velocities were measured at least 0.85 cm from the walls. Indeed, wall effects should have been less important for the larger microspheres, due to their greater velocities and higher R_e. Another possibility is that observed velocities were biased downward by the loss of the fastest values, as the motion analysis system could not process velocities exceeding a certain value. However, we attempted to correct for this by discarding the few particles large enough to fall at velocities exceeding this limit. While the anomalous behavior of the 49-μm microspheres remains unexplained, their observed velocities still serve to "calibrate" the chamber and establish an upper limit on particle sizes for which our apparatus provides results consistent with fluid-dynamic theory.

Conidia of *C. thromboides* appeared to fall at velocities predicted by Stokes' Law, suggesting that although they are not perfectly spherical, they behave aerodynamically very much like spheres having a diameter equal to the average of a spore's length and width. Their size, 17–26 μm, was well within the range for which the polystyrene microspheres also followed Stokes' Law. The larger conidia of *C. obscurus,* although similar in shape to those of *C. thromboides,* fell more slowly than expected. It is possible that the same unknown factors responsible for the irregular behavior of the 49-μm microspheres were also at work here, although the spores were considerably smaller than the microspheres. It is interesting that if the width of *C. obscurus* spores, rather than $(L + W)/2$, was used to represent their diameter, then observed and expected velocities were in close agreement. It may be that the relatively small basal papilla of these conidia (Fig. 1C) contributes very little to their aerodynamic size and should be neglected. Why this should not also be the case for *C. thromboides* is unknown, but may be related to their different sizes, settling velocities, and Reynolds numbers, or to some difference in their settling orientation or behavior.

The ellipsoidal conidia of *Z. radicans* fell with median observed velocities well predicted by Stokes' Law, but for both isolates there was greater variation in velocity than could be explained by the measured variation in size. This excess size dependency could not be explained solely by the slight difference in shape of large and small spores. The most likely cause is the way in which observations were taken from the video fields. Parameters of the video processor were adjusted to eliminate particles whose velocities were less than or greater than certain values. The intent was to eliminate extraneous small objects, such as dust, droplets, and cellular fragments, and large objects, presumably aggregates of two or more spores. The threshold velocities were chosen somewhat arbitrarily, as there were no distinct boundaries, and conservatively, so as to err on the side of inclusion. Thus, the parameters used may have admitted some low and high velocities not representing single conidia. We attempted to exclude aggregates by discarding any velocities that were greater than that expected of the largest measured spore. However, calculations show that the remaining observations may still have included aggregates of two small conidia, whose velocity as a unit would still be less than that of a single large spore.

Conidia of *Z. radicans* always oriented vertically while settling in still air and exhibited very stable aerodynamic behavior. As a consequence, little or no correction for shape was called for when computing

expected velocities. How spores would orient in moving, especially turbulent, air is unknown, as is the effect that spore shape would have on aerial dispersal under natural conditions. We speculate that in disturbed air spores might assume random orientations, with a net reduction in mean settling velocity (Davies, 1964; Fuchs, 1964). The uniformly vertical orientation we observed in the settling chamber deserves comment. Symmetrical, uniformly dense, elongate particles are expected to retain whatever initial orientation they might have had as they settle at very low R_e ($R_e < 0.05$–0.1), or to orient with the long axis horizontal at higher R_e. Conidia of *Z. radicans* are essentially symmetrical (Fig. 1A), although they have a basal papilla with a delimiting ridge (Waterhouse and Brady, 1982). Interference microscopy has revealed that the basal end of the conidium is more dense than the apical end (data not shown), which should cause the spore to fall basal end downward. However, we were unable to tell from the video images which way conidia oriented. Vertical orientation of ellipsoidal conidia of the powdery mildew fungus, *Erysiphe graminis* (13×32 μm) has been noted, and was attributed to displacement of the center of gravity, rotation about the axis of symmetry, or wall effects (Yarwood and Hazen, 1942). The apparent oscillations of ± 0.5–$5°$ we observed in the falling orientation of some conidia may have represented rotation or autogyration, but such rapid motions (15–30 cycles sec^{-1}) are not expected at low R_e because of the dominance of viscous forces (Niklas, 1992, p. 446). The cause of the apparent oscillations is unknown.

The size and density of entomophthoralean conidia are comparable to those of other fungal spores and pollen grains, suggesting that passive aerial dispersal may play as important a role in their life cycles, ecology, and epidemiology as it does for other organisms. The aerodynamics of these small structures are dominated by viscous forces, in which boundary layers of air form sticky barriers over surfaces, and motion within parcels of still air is slow and steady, if ever-downward. This last condition has one important exception: the brief moment of violent discharge when conidia are ejected from the boundary layer covering the parent mycelium and enter the surrounding air space. What happens next depends on local environmental conditions. If the insect host has died in an exposed location, conidia may be transported considerable distances by moving air (Wilding, 1970). Although the force of gravity ensures that particles are continually falling within the small volume of air in which they exist, the unit of air itself may be moving horizontally or even upward, carrying spores with it. Whether or not these spores contribute to the development of an epidemic, and at what distance, depends on the outcome of a sequence of processes including transport, dilution, survival, and deposition (Aylor, 1986). A consequence of the small size of conidia is that their movement is highly sensitive to fluctuations of wind speed of a magnitude similar to their own terminal velocities, at most a few centimeters per second (Burrows, 1986). Variations in physical properties of the spore may have only a minor influence on transport, but are very important factors in deposition. Here, viscous forces play a major role, and the size, shape, density, adhesiveness, and surface charge of conidia determine the magnitude and relative importance of sedimentation, impaction, boundary layer exchange, turbulent deposition, precipitation scrubbing, and electrostatic deposition (Davies, 1966b; Chamberlain, 1967; Gregory, 1973). The spatial structure of vegetation, including its height, density, and the type and orientation of leaves, influences the wind profile and the nature of turbulence within a canopy and its effectiveness as a filter of airborne particles.

The information obtained in the present study is the first of its kind obtained for entomophthoralean conidia. Basic measurements of spore size, shape, density, settling velocity, and aerodynamic behavior provide a foundation for the development of models of aerial transport of entomophthoralean conidia. Additional information is needed on conidial survival in air at different relative humidities, on air movement and moisture conditions in and above canopies during and after periods of sporulation, and on deposition of spores on plant and soil surfaces. Taken together, these data will allow us to apply existing models of particulate transport to the problem of aerial dissemination of entomopathogenic fungi and to gain a better understanding of the spatial dynamics of these important microbial agents of insect disease.

ACKNOWLEDGMENTS

We gratefully acknowledge the expert advice of Karl Niklas, who cautioned us about wall effects and suggested calibrating the settling chamber with microspheres. We thank Donald Aylor, Richard Humber, Guy Knudsen, and Stuart Krasnoff for reviewing the manuscript. Mark Specht, of Spectra Services, Inc., provided technical advice on video equipment. Donna Gibson led us to Bangs Laboratories, Inc., who provided samples of polystyrene microparticles. This research was supported in part by grants from NASA and USDA–CSRS (Hatch funds) to R.W.

Mention of a commercial or proprietary product does not constitute an endorsement or recommendation for its use by USDA.

REFERENCES

Aylor, D. E. 1975. Deposition of particles in a plant canopy. *J. Appl. Meteorol.* 14, 52–57.

Aylor, D. E. 1978. Dispersal in time and space: Aerial pathogens. *In* "Plant Disease: An Advanced Treatise" (J. G. Horsfall, and E. B. Cowling, Eds.), Vol. 2, pp. 159–180.

Aylor, D. E. 1986. A framework for examining inter-regional aerial transport of fungal spores. *Agric. For. Meteorol.* 38, 263–288.

Aylor, D. E. 1990. The role of intermittent wind in the dispersal of fungal pathogens. *Annu. Rev. Phytopathol.* 28, 73–92.

Aylor, D. E., and Ferrandino, F. J. 1989. Temporal and spatial development of bean rust epidemics initiated from an inoculated line source. *Phytopathology* 79, 146–151.

Barer, R., and Joseph, S. 1958. Concentration and mass measurements in microbiology. *J. Appl. Bacteriol.* 21, 146–159.

Beckett, A., Read, N. D., and Porter, R. 1984. Variations in fungal spore dimensions in relation to preparatory techniques for light microscopy and scanning electron microscopy. *J. Microsc.* 136, 87–95.

Berger, R. D., and Luke, H. H. 1979. Spatial and temporal spread of oat crown rust. *Phytopathology* 69, 1199–1201.

Brobyn, P. J., Wilding, N., and Clark, S. J. 1987. Laboratory observations on the effect of humidity on the persistence of infectivity of conidia of the aphid pathogen *Erynia neoaphidis*. *Ann. Appl. Biol.* 110, 579–584.

Burrows, F. M. 1986. The aerial motion of seeds, fruits, spores and pollen. *In* "Seed Dispersal" (D. R. Murray, Ed.), pp. 1–47. Academic Press, New York.

Carruthers, R. I., and Soper, R. S. 1987. Fungal diseases. *In* "Epizootiology of Insect Diseases" (J. R. Fuxa, and Y. Tanada, Eds.), pp. 357–416. Wiley, New York.

Chamberlain, A. C. 1967. Deposition of particles to natural surfaces. *In* "Airborne Microbes: 17th Symposium Soc. General Microbiol" (P. H. Gregory, and J. L. Monteith, Eds.), pp. 138–164. Cambridge Univ. Press, Cambridge, England.

Chamberlain, A. C., and Chadwick, R. C. 1972. Deposition of spores and other particles on vegetation and soil. *Ann. Appl. Biol.* 74, 141–158.

Chatigny, M. A., Dimmick, R. L., and Harrington, J. B. 1979. Deposition. *In* "Aerobiology: The Ecological Systems Approach" (R. L. Edmonds, Ed.), US/IBP Synthesis Series 10, pp. 111–150. Dowden, Hutchinson & Ross, Stroudsburg, PA.

Davies, C. N. 1964. Shape of small particles. *Nature (London)* 201, 905–907.

Davies, C. N. (Ed.). 1966a. "Aerosol Science." Academic Press, London.

Davies, C. N. 1966b. Deposition from moving aerosols. *In* "Aerosol Science" (C. N. Davies, Ed.), pp. 393–446. Academic Press, New York.

de Jong, M. D., Wagenmakers, P. S., and Goudriaan, J. 1991. Modelling the escape of *Chondrostereum purpureum* spores from a larch forest with biological control of *Prunus serotina*. *Neth. J. Plant Pathol.* 97, 55–61.

Di-Giovanni, F., Beckett, P. M., and Flenley, J. R. 1989. Modelling of dispersion and deposition of tree pollen within a forest canopy. *Grana* 28, 129–139.

Dwyer, G. 1992. On the spatial spread of insect pathogens: Theory and experiment. *Ecology* 73, 479–494.

Entwhistle, P. F., Adams, P. H. W., Evans, H. F., and Rivers, C. F. 1983. Epizootiology of a nuclear polyhedrosis virus (Baculoviridae) in European spruce sawfly (*Gilpinia hercyniae*): Spread of disease from small epicentres in comparison with spread of baculovirus diseases in other hosts. *J. Appl. Ecol.* 20, 473–487.

Fitt, B. D. L., Gregory, P. H., Todd, A. D., McCartney, H. A., and Macdonald, O. C. 1987. Spore dispersal and plant disease gradients; a comparison between two empirical models. *J. Phytopathol.* 118, 227–242.

Fuchs, N. A. 1964. "The Mechanics of Aerosols." Pergamon, Oxford.

Glare, T. R., and Milner, R. J. 1991. Ecology of entomopathogenic fungi. *In* "Handbook of Applied Mycology. Vol. 2. Humans, Animals, and Insects" (D. K. Arora, L. Ajello, and K. G. Mukerji, Eds.), pp. 547–612. Marcel Dekker, New York.

Green, H. L., and Lane, W. R. 1964. "Particulate Clouds: Dust, Smokes and Mists". Van Nostrand, Princeton, NJ.

Gregory, P. H. 1945. The dispersion of air-borne spores. *Trans. Br. Mycol. Soc.* 28, 26–72.

Gregory, P. H. 1973. "The Microbiology of the Atmosphere", 2nd ed. Wiley, New York.

Gregory, P. H., and Monteith, J. L. (Eds.). 1967. "Airborne Microbes. 17th Symposium Soc. General Microbiol., Imperial College, London April 1967." Cambridge Univ. Press, Cambridge, England.

Humber, R. A. (Ed.). 1992. "USDA-ARS Collection of Entomopathogenic Fungal Cultures. Catalog of Strains." USDA–ARS, Plant Protection Research Unit, Ithaca, New York.

Ingold, C. T. 1971. "Fungal Spores: Their Liberation and Dispersal." Clarendon, Oxford.

Jeger, M. J. (Ed.). 1989. "Spatial Components of Plant Disease Epidemics." Prentice Hall, Englewood Cliffs, NJ.

Latgé, J. P., Perry, D. F., Prévost, M. C., and Samson, R. A. 1989. Ultrastructural studies of primary spores of *Conidiobolus, Erynia,* and related Entomophthorales. *Can. J. Bot.* 67, 2576–2589.

Legg, B. J., and Powell, F. A. 1979. Spore dispersal in a barley crop: A mathematical model. *Agric. Meterol.* 20, 47–67.

Leonard, K. J., and Fry, W. E. (Eds.). 1986. "Plant Disease Epidemiology. Vol. 1. Population Dynamics and Management." Macmillan, New York.

MacLeod, D. M. 1963. Entomophthorales infections. *In* "Insect Pathology: An Advanced Treatise" (E. A. Steinhaus, Ed.), Vol. 2, pp. 189–0. Academic Press, New York.

Matsumoto, N., and Tajimi, A. 1985. Convergence in spore size of air-borne obligate plant parasitic fungi. *Trans. Mycol. Soc. Jpn* 26, 261–267.

McCabe, D. E., and Soper, R. S. 1985. Preparation of an entomopathogenic fungal insect control agent. U.S. Patent 4,530,834.

McCartney, H. A. 1991. Airborne dissemination of plant fungal pathogens. *J. Appl. Bacteriol. Symposium Suppl.* 70, 39–48.

McCartney, H. A., and Bainbridge, A. 1987. Deposition of *Erysiphe graminis* conidia on a barley crop. I. Sedimentation and impaction. *J. Phytopathol.* 118, 243–257.

McCartney, H. A., and Fitt, B. D. L. 1985. Construction of dispersal models. *In* "Mathematical Modelling of Crop Disease, Vol. 3, Advances in Plant Pathology" (C. A. Gilligan, Ed.), pp. 107–143. Academic Press, New York.

Meredith, D. S. 1973. Significance of spore release and dispersal mechanisms in plant disease epidemiology. *Annu. Rev. Phytopathol.* 11, 313–342.

Niklas, K. J. 1992. "Plant Biomechanics: An Engineering Approach to Plant Form and Function." Univ. Chicago Press, Chicago.

Okubo, A., and Levin, S. A. 1989. A theoretical framework for data analysis of wind dispersal of seeds and pollen. *Ecology* 70, 329–338.

Onstad, D. W., and Maddox, J. V. 1989. Modeling the effects of the microsporidium *Nosema pyrausta* on the population dynamics of the insect *Ostrinia nubilalis*. *J. Invertebr. Pathol.* 53, 410–421.

Parkin, C. S., and Merritt, C. R. 1988. The measurement and prediction of spray drift. *Aspects Appl. Biol.* 17, 351–361.

Tanada, Y. 1963. Epizootiology of infectious diseases. *In* "Insect Pathology: An Advanced Treatise" (E. A. Steinhaus, Ed.), Vol. 2, pp. 423–475. Academic Press, New York.

Thaxter, R. 1888. The Entomophthoraceae of the United States. *Mem. Boston Soc. Nat. Hist.* 4, 133–201.

Uziel, A., and Kenneth, R. G. 1991. Survival of primary conidia and capilliconidia at different humidities in *Erynia* (subgen. *Zoophthora*) spp. and in *Neozygites fresenii* (Zygomycotina, Entomophthorales), with special emphasis on *Erynia radicans*. *J. Invertebr. Pathol.* 58, 118–126.

Vogel, S. 1981. "Life in Moving Fluids: The Physical Biology of Flow." Princeton University Press, Princeton, NJ.

Waterhouse, G. M., and Brady, B. L. 1982. Key to the species of *Entomophthora* sensu lato. *Bull. Br. Mycol. Soc.* 16, 113–143.

Wayne, R., and Staves, M. P. 1991. The density of the cell sap and endoplasm of *Nitellopsis* and *Chara*. *Plant Cell Physiol.* 32, 1137–1144.

Weast, R. C. (Ed.). 1983. "CRC Handbook of Chemistry and Physics," 64th ed. CRC Press, Boca Raton, FL.

Webster, J., Proctor, M. C. F., Davey, R. A., and Duller, G. A. 1988. Measurement of the electrical charge on some basidiospores and an assessment of two possible mechanisms of ballistospore propulsion. *Trans. Br. Mycol. Soc.* 91, 193–203.

White, C. M. 1946. The drag of cylinders in fluids at low speeds. *Proc. R. Soc. London Series A* 186, 472–479.

Wilding, N. 1970. *Entomophthora* conidia in the air-spora. *J. Gen. Microbiol.* 62, 149–157.

Yarwood, C. E., and Hazen, W. E. 1942. Vertical orientation of powdery mildew conidia during fall. *Science* 96, 316–317.

Zadoks, J. C., and Schein, R. D. 1979. "Epidemiology and Plant Disease Management." Oxford Univ. Press, London.